

1
2
3
4
5
6
7
8
9

Evaluation of the battery operation in ramp-rate control mode within a PV plant: A case study

S. A. Pourmousavi^{a,*}, Tapan Kumar Saha^b

^a*Global Change Institute, University of Queensland, Brisbane, QLD 4072, Australia*

^b*School of Information Technology and Electrical Engineering, University of Queensland, Brisbane, QLD 4072, Australia*

Abstract

Spatial and temporal variability of PV generation is a challenge for secure operation of the power systems. Several solutions are already proposed to deal with this issue. Among the proposed solutions, storage technologies (particularly battery) attracted more attention as a promising solution for the application in medium- and large-scale PV plants. While numerous research studies addressed optimal sizing and real-time operation of the storage systems in such applications, there is no study on the battery operation assessment in real-world application based on field data. In this paper, one year of experimental data from a 3.275 MWp PV plant with 600kW/760kWh Li-Polymer battery system is examined from different perspectives (e.g., battery energy, power, rate of change of power (RoCoP), and state-of-charge (SOC)) to draw insights from battery operation within the plant. The field data inherently contains system-wide losses, smoothing effect of the PV plant, and PV inverter operation for reactive power control, which provides a realistic as-

*Corresponding author

Email addresses: a.pour@uq.edu.au (S. A. Pourmousavi), saha@itee.uq.edu.au (Tapan Kumar Saha)

1
2
3
4
5
6
7
8
9 assessment. Furthermore, several operational parameters (such as energy and
10 power during ramp events) are evaluated and modelled using appropriate
11 statistical tools based on experimental data. In addition, a simple super-
12 capacitor sizing study is carried out to reveal the effectiveness of a hybrid
13 energy solution for such applications. Observations and insights drawn from
14 the proposed analyses will help future research on the battery sizing and op-
15 eration to effectively account for real-world characteristics and requirements.
16
17

18 *Keywords:* Medium-scale PV and battery system, seasonality effect,
19 smoothing, ramp-up and ramp-down, statistical modelling

20
21
22
23
24 **1. Introduction**
25
26
27

28 According to the Australian PV Institute (APVI) [1], installed PV capac-
29
30 ity reached 5,855.6MW by January 2017 in Australia, which shows more than
31
32 61 times growth compared to January of 2010 (when total installed capacity
33
34 was 95.7MW). While the number of small-scale PV installation is gradu-
35
36 ally dropping [1], the number of medium- and large-scale PV systems, i.e.,
37
38 100kW~5MW and bigger than 5MW respectively, has been growing steadily
39
40 in Australia in recent years. Only in 2016, 68 medium-scale and 12 large-scale
41
42 solar projects with total capacity of 23MW and 319MW, respectively, were
43
44 commissioned in the country [2]. While increasing PV generation can bene-
45
46 fit the country in several ways, technical challenges regarding power system
47
48 operation raised serious concerns, which have to be appropriately addressed
49
50 [3, 4]. Among all detrimental impacts, variability of PV output power due
51
52 to passing clouds (known as ramp-rate) is the one of paramount importance
53
54 for frequency and voltage regulation of power system with high PV genera-
55
56
57

1
2
3
4
5
6
7
8
9 16 tion [5]. To reduce the negative impacts of the medium- and large-scale PV
10 17 plants, electricity utilities imposed obligatory connection rules, such as ramp-
12 18 rate and voltage violations limit, as a part of interconnection agreement [6, 7].
14 19 Any failure to meet the requirements could have financial consequences for
16 20 the plant owners/operator.

18 21 To address the PV variability problem, researchers proposed various ap-
19 22 proaches and techniques to control rapid changes in PV production, as sum-
20 23 marised in [8]. While distributing panels over a wide area can smooth ramp
21 24 effects, it is not going to resolve the issue completely, as will be shown in
22 25 this paper. Power-electronic-based control techniques are also developed
23 26 in literature to smooth PV output fluctuations within short-time intervals
24 27 [9, 10]. These approaches, however, cannot compensate ramp events with
25 28 high energy and power due to technical limitations of power electronic inter-
26 29 faces. Most recent solutions are mainly focused on the application of various
27 30 storage technologies (specifically battery) for medium- and large-scale PV
28 31 ramp compensation. Optimal and intelligent algorithms are proposed in
29 32 [11, 12, 13, 14, 15, 16, 17, 18] to operate battery in ramp-rate control mode .
30 33 Also, storage sizing for PV ramp-rate control has been reported in multiple
31 34 papers, e.g., in [19, 20]. In these studies, the mathematical model of a single
32 35 PV module is used to generate PV power time series to further calculate
33 36 ramp-rates in different time resolution. In addition, pure simulation studies
34 37 were mainly employed to assess battery operation under the ramp-rate reg-
35 38 ulation mode. To the best of our knowledge, however, there is no research
36 39 study that looked into battery operation in ramp-rate control mode using
37 40 field data.

1
2
3
4
5
6
7
8
9 In this paper, operational data from a 3.275 MWp PV plant with 600kW/760kWh
10
11 Li-Polymer battery system is utilised for analyses from different perspectives.
12
13 The PV plant is located at the University of Queensland (UQ) Gatton cam-
14 pus, Australia. The plant with battery system is in operation for more than
15 a year and a half. The battery system is operated by a central supervisory
16 controller in different modes based on pre-defined rules. One of the battery
17 operation modes, which is considered in this study, is designed to compen-
18 sate quick drop in the PV output in real-time. Despite other research studies,
19 where mathematical models and simulation framework were used to identify
20 ramp requirements, actual ramp incidents from the PV modules and battery
21 response to the events are investigated in this study. Therefore, real-world
22 operational characteristics of the plant, such as system-wide losses, inverter's
23 operation for smoothing PV output and reactive power control, PV module
24 degradation, etc., are represented in the experimental data and consequently
25 in the analyses. To shed light on the battery operation in the ramp-rate
26 control mode, this paper offers a thorough evaluation of battery operational
27 behaviour in terms of energy, power, rate of change of power (RoCoP), and
28 battery state-of-charge (SOC). Additionally, time gap between consecutive
29 ramp events, which have been compensated by the battery, are analysed to
30 identify technical requirements in real-world operational conditions. Season-
31 ality effect on the ramping events is also investigated and statistical behaviour
32 of the battery operation is derived from the experimental data. The key find-
33 ings of the analyses can be used in the future battery sizing and operation
34 studies to account for stochastic nature of the underlying system. To show
35 the effectiveness of the hybrid energy storage system in ramp-rate control
36
37
38
39
40
41
42
43
44
45
46
47
48
49
50
51
52
53
54
55
56
57
58
59
60
61
62
63
64
65

1
2
3
4
5
6
7
8
9 66 mode, a simple super-capacitor sizing study carried out. It is shown that
10 67 low-energy incidents (which often coincide with low-power events) can be
11 68 conveniently mitigated by super-capacitor. This will, in turn, help to extend
12 69 battery lifetime and improve economic operation of the whole plant. Ulti-
13 70 mately, ramping incidents on the DC and AC sides of the PV inverters are
14 71 assessed for a year of field data. As a result, a set of new requirements are
15 72 identified, which will have implications on the future research in this area.

16
17 73 The rest of the paper is organised as follows. Section 2 explains sys-
18 74 tem under study including the plant control mechanism and interconnection
19 75 agreement with the local utility. In Section 3, a general overview of the bat-
20 76 tery operation under ramp-rate control is presented. Moreover, statistical
21 77 tools and concepts, which have been used for the analyses, are outlined and
22 78 explained in this section. Battery operation is then evaluated from different
23 79 perspective in Section 4. Finally, paper is concluded in Section 5.

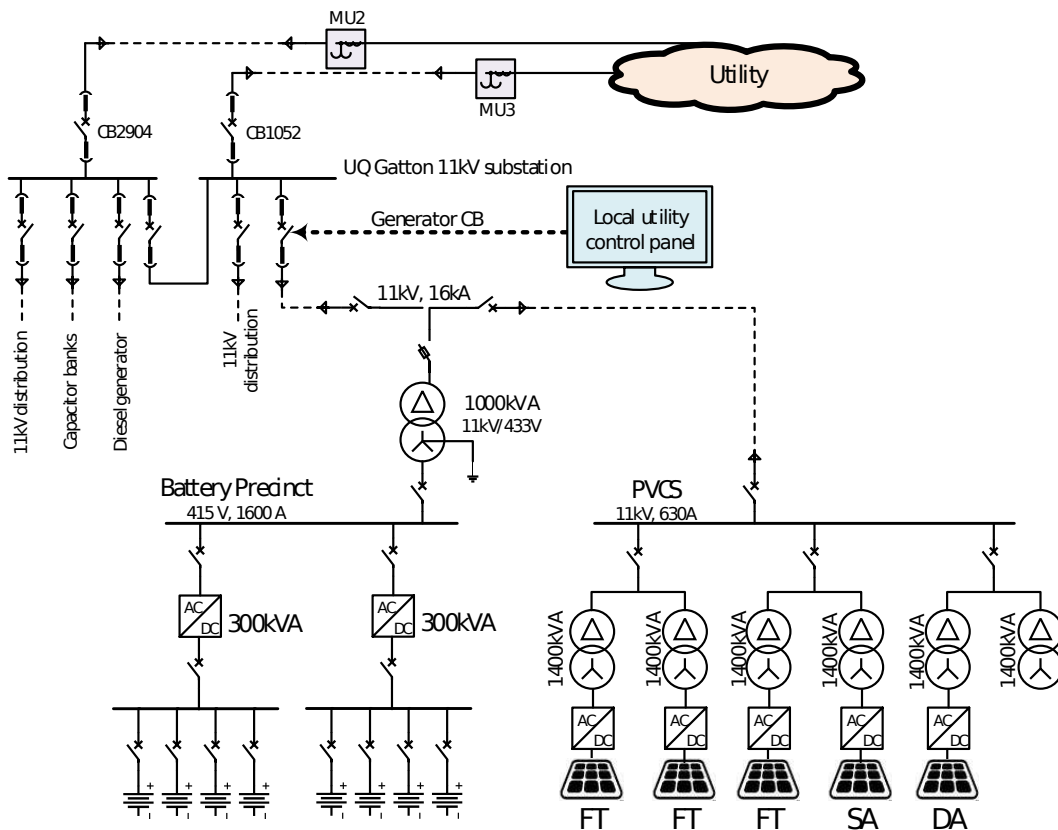
24
25
26
27
28
29
30
31
32
33
34 80 **2. System Under Study**

35
36
37
38
39
40 81 The UQ owns and operates a 3.275 MWp PV plant along with 600kW/760kWh
41
42 82 battery system at the Gatton campus, located in the Lockyer Valley region
43
44 83 of South East Queensland, Australia. A schematic diagram of the plant is
45
46 84 shown in Fig. 1, in connection to the UQ Gatton substation and local util-
47
48 85 ity grid. The UQ Gatton 11-kV substation has two complementary parts.
49
50 86 Onsite diesel generator (1MVA), capacitor banks (2×550 kVAr), and most of
51
52 87 campus loads are connected to the left busbar. Power can flow between the
53
54 88 two busbars through a normally closed circuit breaker, as shown in Fig. 1.
55
56 89 The campus load is served by onsite PV generation and storage as well as

utility grid. Excess PV generation, when available, is exported to the grid using the same circuit. As it is shown in Fig. 1, there are five PV arrays, three of them are fixed-tilt (FT) arrays (684KWp DC each), one array with single-axis (SA) tracking system (684KWp DC), and the fifth array with dual-axis (DA) tracking mechanism (684KWp DC). Each array is linked to the substation through an exclusive inverter, which is limited to deliver 630 kW AC at any moment of time. Interested readers are referred to [21] for more detail on the plant operation.

Li-Polymer batteries are installed in the plant. As shown in Fig. 1, battery power/energy capacity is divided into two 300kW/380kWh banks, each of which is connected to a 300kVA, 415V, 3-phase inverter capable of sourcing/sinking reactive power at ± 0.9 power factor. The two inverters are connected to the campus substation through a single 1000kVA transformer. Each battery bank consists of four racks in parallel, as shown in Fig. 1, where 10 battery modules are assembled in series in every rack. Every module contains two parallel strings, where each string has 18 battery cells in series. Voltage at the DC side of the battery inverter varies between 576 and 748 V based on the battery SOC and internal resistances. As expected, several constraints are defined for battery operation in the central supervisory system (CSS). For instance, battery SOC is strictly limited between 15% and 95%. The CSS operates the whole plant consisting of PV arrays, battery storage system, diesel generator, capacitor banks, and local grid connection. A comprehensive SCADA system is implemented to measure, collect, and communicate data within the plant, which is essential for the CSS operation. More details about smart metering and data collection in the plant can be

115 found in [21].



39
40 Figure 1: Single-line diagram of the Gatton PV plant and local network interconnection
41
42
43

44 *2.1. Agreement with the Local Utility*
45

46 According to the agreement, PV inverters are limited to export 630 kW
47
48 Additionally, they are required to regulate reactive power such that at
49
50 30% or more of the rated inverter output, the amount of reactive power is
51
52 at least 0.395 times the active power output [21]. This way, “Ramp Mode”
53
54 is defined for the PV inverters to regulate ramp-up events [21]. There are
55
56 multiple agreement on the voltage level and violations, which are not related
57
58

1
2
3
4
5
6
7
8
9 123 to battery operation, and not discussed in this paper.
10
11

12 124 *2.2. Battery Control Mechanism*
13

14 125 Battery, similar to other devices in the plant, is monitored and controlled
15 126 by the CSS directly. In particular, ten operation modes (rules) are defined for
16 127 the battery with predefined priorities. **Delta Solar**, as one of the operation
17 128 rules, is activated when solar power reduction exceeds a certain level. Battery
18 129 contribution to the compensation of ramp-down events decreases slowly when
19 130 solar power generation stables at a certain level. This summarises ramp-down
20 131 control mechanism provided by the battery. In **Solar Charge** mode, on the
21 132 other hand, battery is charged when PV generation exceeds 800kW during
22 133 certain hours of each day. This is not exactly ramp-up control as it operates
23 134 based on the magnitude of the PV generation rather than the change in
24 135 the PV output. Other battery modes are not related to either ramp-up or
25 136 ramp-down events. Besides battery system, as explained in subsection 2.1,
26 137 PV inverters are setup to limit extreme ramp-up events. Therefore, battery
27 138 does not contribute in regulating ramp-up incidents in the Gatton plant. As
28 139 a result, battery performance will only be studied during ramp-down events
29 140 in this study.
30
31
32
33
34
35
36
37
38
39
40
41
42
43
44
45
46
47
48
49
50
51
52
53
54
55
56
57
58
59
60
61
62
63
64
65

141 **3. Overview of the Battery Operation and Analysis**

142 In this section, a general overview of the battery operation during ramp-
143 down events is given for one year of field data. Then, statistical terms and
144 methods, which have been used in Section 4, are explained.

1
2
3
4
5
6
7
8
9 145 *3.1. General Overview of the Ramp-Down Control Mode*

10
11 146 As it was explained in subsection 2.2, **Delta Solar** mode is activated
12 147 during ramp-down events of 10kW/s or higher. While the CSS regulates
13 148 plant operation in second-by-second basis, our analyses are carried out for
14 149 minute-by-minute data for practical reasons (such as memory management
15 150 and tractable computational requirements). Data are averaged every minute
16 151 and relevant parameters are converted, when needed. For instance, ramp-
17 152 down event is re-defined as 600kW/min (instead of 10kW/s) or larger reduc-
18 153 tion of the PV generation. One year of the battery operation data starting
19 154 from 1st of March 2016 is utilised for analysis. For simplicity, data for one
20 155 battery bank is assessed because the two banks show almost identical be-
21 156 haviour throughout the year.

22
23 157 In total, battery was discharged in **Delta Solar** mode for 7,928 minutes
24 158 (equivalent of 11 days, 19 hours, and 46 minutes accumulatively) throughout
25 159 the year. Total energy discharged from the battery during this time was
26 160 about 12.9 MWh per bank. This equals to 21.3 full cycles (based on the
27 161 installed capacity of the battery bank and 80% rated Depth-of-Discharge
28 162 (DoD)) cumulatively during discharging mode, calculated as follows:

29
30
31
32
33
34
35
36
37
38
39
40
41
42
43
44
45
46
47
48
49
50
51
52
53
54
55
56
57
58
59
60
61
62
63
64
65

$$\text{Cycles} = (2 \times DoD \times E_{rated})^{-1} \times \sum_{i=1}^{7928} |P_i| \times \frac{1}{60} \quad (1)$$

50 163 where P_i is the discharge power in i^{th} time instance in kW for battery bank
51 164 1; DoD is the rated DoD of the battery (0.8 p.u.); and E_{rated} is the rated ca-
52 165 pacity of the battery bank 1 in kWh (380 kWh). From the annual operation
53 166 point of view, 21 cycles per year is insignificant, which justifies stacked appli-
54 167 cation of the battery in such systems. From the battery operation standpoint,

1
2
3
4
5
6
7
8
9 168 however, this means that the battery undergone almost 1.8 cycles per day
10 169 in **Delta Solar** mode, i.e., 21.3 cycles in almost 12 days. This is relatively
11 170 intense as the battery at the UQ Gatton plant experiences about half a cycle
12 171 on average per day. It further shows that battery capable of deep cycling
13 172 with high power, such as Li-based technologies, are needed for the PV ramp-
14 173 rate control application. In Section 4, significance of different parameters on
15 174 battery operation during **Delta Solar** mode will be investigated thoroughly.
16
17
18
19
20
21
22
23
24
25
26
27
28
29
30
31
32
33
34
35
36
37
38
39
40
41
42
43
44
45
46
47
48
49
50
51
52
53
54
55
56
57
58
59
60
61
62
63
64
65

175 *3.2. Analysis Methods and Definitions*

176 In this paper, different statistical tools and concepts are used to perform
177 the analyses. While average and standard deviation (SD) are calculated for
178 the experimental data to compare performance and operational stress on the
179 battery in different circumstances, Skewness and Kurtosis are computed to
180 characterise the stochastic nature of the data and detect potential outliers.
181 More specifically, skewness is used as a measure of asymmetry of any density
182 and probability distribution of a random variable about its mean [22]. The
183 skewness value can be positive or negative, or undefined. For a unimodal
184 distribution (i.e., a distribution with only one clear-cut peak), negative skew
185 indicates that the tail on the left side of the probability density function
186 is longer or fatter than the right side. Non-zero skewness means that the
187 random variable is not following a normal distribution [22]. Therefore, it
188 would be a mistake to statistically model such random variables with normal
189 distribution. Kurtosis is a descriptor of the shape of a distribution. Higher
190 kurtosis is a sign of rare extreme deviations (or outliers), as opposed to
191 frequent reasonably-sized deviations [22]. The sample kurtosis is a useful
192 measure of whether there is a problem with outliers in a data set. Larger

1
2
3
4
5
6
7
8
9 193 kurtosis indicates existence of a serious outlier, which is recommended to be
10 194 removed from dataset.

13 195 Modelling statistical behaviour of random parameters are very useful in
14 196 sizing studies and developing operational algorithms for battery. These mod-
15 197 els can be applied to account for stochastic nature of the battery operation in
16 198 such studies. Since ramp events are random in nature, they can be modelled
17 199 by finding appropriate density or probability distribution for given exper-
18 200 imental data. To find the best distribution (either frequency or probabil-
19 201 ity) for a given set of data, a measure of comparison is needed. In this
20 202 paper, corrected Akaike Information Criterion (AICc) [22] is used which is
21 203 corrected AIC for sample size, i.e., it is independent of the sample size. It is
22 204 an information-based criteria that assess model fit based on -2Log-Likelihood
23 205 [22]. While AICc can help to find the best distribution for a set of data, it
24 206 is not able to determine the accuracy of the fitted distribution. Therefore,
25 207 quantile-quantile plot (Q-Q Plot) is used to visually verify the validity of the
26 208 best fit on the experimental data [23]. In a Q-Q plot, theoretical expected
27 209 values will be computed based on the fitted distribution function on x-axis
28 210 and the results are compared with the experimental values on Y axis. If the
29 211 experimental data truly follow the distribution, points on the Q-Q plot will
30 212 follow a straight line.

33 213 Frequency histograms are also used to draw insights from experimental
34 214 data. Selecting appropriate number of bins in a histogram, which further
35 215 defines the width of the bins, is critical for data with outliers. In this study,
36 216 number of bins in a histogram is selected based on Freedman-Diaconis rule
37 217 [24], which is less sensitive to outliers in the data and more suitable for

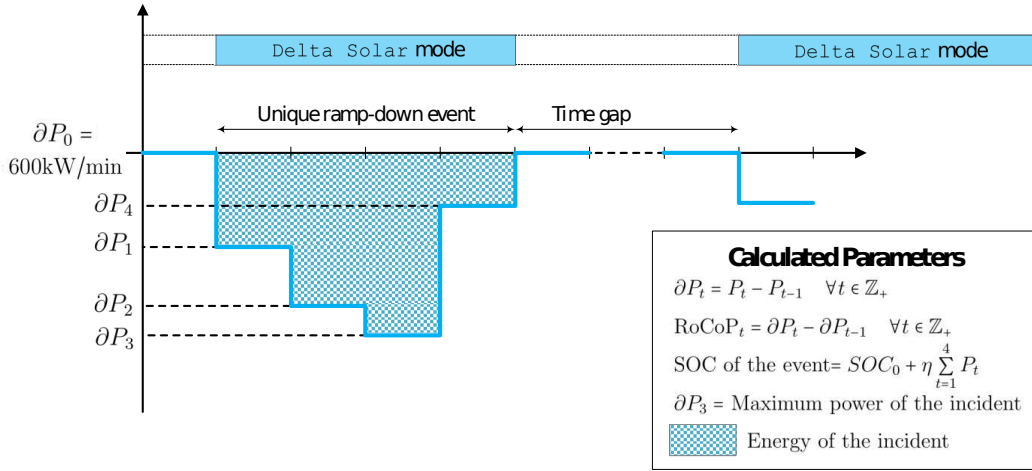
1
2
3
4
5
6
7
8
9 218 heavy-tailed distributions. The optimal bin-width is calculated by:
10
11
12
13

$$h = 2 \times IRQ \times n^{-1/3} \quad (2)$$

14
15 219 where IRQ is the interquartile range of data; and n is the number of samples.
16
17 220 Then, optimal number of bins is:
18
19
20
21

$$N = (max^{data} - min^{data})/h \quad (3)$$

221 The tools and concepts, explained in this subsection, are used in the next
222 section to evaluate battery operation and performance in ramp-rate control
223 mode. The analyses will lead to identify useful insights for the battery sizing
224 and operation studies during ramp-down control within a medium-scale PV
225 plant.
32
33
34
35 226 **4. Battery Operation Analysis**
36
37
38 227 In this section, battery operation is evaluated from different perspectives
39 using available data through various statistical methods. Please note that
40
41 229 all the analyses in this section have been done for one battery bank. Similar
42 observations can be extended to the second battery bank. Different param-
43
44 231 ters are calculated based on the raw data, which are shown for a hypothetical
45 ramp-down event in Fig. 2. ∂P_t is the ramp value in kW/min: and $RoCoP_t$
46
47 232 is the RoCoP at time t . The concept of “unique ramp-down event”, “en-
48
49 233 ergy of the incident”, “maximum power of the incident”, “SOC at the end of
50
51 234 the incident”, and “time gap” between consecutive events are illustratively
52
53 235 shown in the figure.
54
55
56
57
58
59
60
61
62
63
64
65



237 4.1. Energy

238 The amount of energy extracted from the battery during ramp-down
 239 events is of paramount importance because it affects battery health and its
 240 readiness for the future incidents. It is also one of the two critical factors (the
 241 other one is ramp-down power) in battery sizing studies in literature, e.g.,
 242 [20, 25]. The general statistics for every unique ramp-down event are reported
 243 in Table 1 for different seasons and annual values. A “unique ramp-down
 244 event” is defined as a sequence of battery discharge with possibly different
 245 level of power without interruption during the **Delta Solar mode**. Based
 246 on the raw data, the maximum annual energy drained from the battery oc-
 247 curred in spring, where battery was discharged for 41 minutes consecutively
 248 to compensate quick drop in the PV generation. This incident drained 163.1
 249 kWh from the battery. It is clear from Table 1 that this event is far bigger
 250 than the next maximum value in the whole dataset as well as within the
 251 samples of spring. Also, the large Skewness and Kurtosis values in spring,

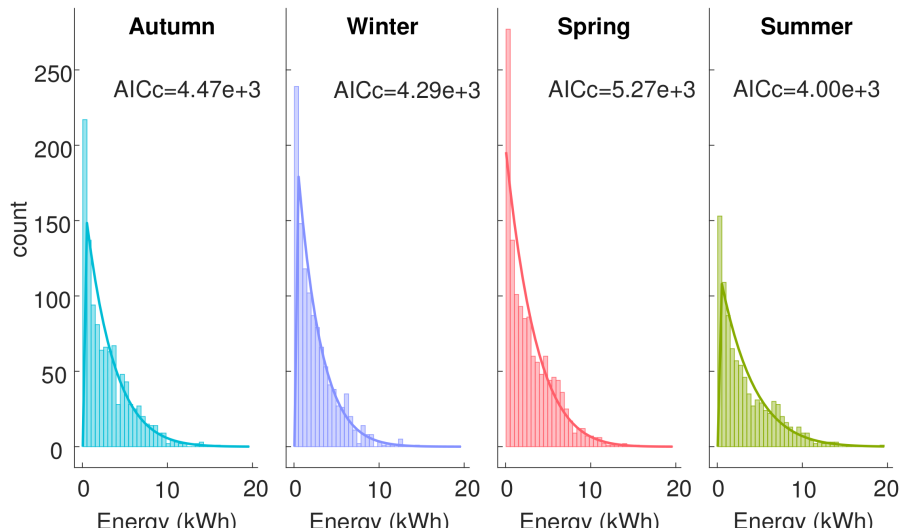
1
 2
 3
 4
 5
 6
 7
 8
 9
 10
 11
 12
 13
 14
 15
 16
 17
 18
 19
 20
 21
 22
 23
 24
 25
 26
 27
 28
 29
 30
 31
 32
 33
 34
 35
 36
 37
 38
 39
 40
 41
 42
 43
 44
 45
 46
 47
 48
 49
 50
 51
 52
 53
 54
 55
 56
 57
 58
 59
 60
 61
 62
 63
 64
 65

252 compared to other seasons, further proves that the event is an outlier in a
 253 statistical sense. It means that although the incident actually took place in
 254 spring, it does not represent typical behaviour of the parameter, as it only
 255 occurs once in a lifetime. In the battery sizing studies, such an event is a
 256 rare incident, where accrued penalty does not justify the cost of an over-sized
 257 battery. Therefore, the incident can be treated as an outlier to be safely re-
 258 moved from the dataset for the rest of the paper. Maximum, average, SD,
 259 Skewness, and Kurtosis of the samples in spring without outlier are given in
 260 parenthesis in Table 1. It can be seen that the new parameters in spring are
 261 reasonably close to the values of other seasons. Also, Kurtosis is significantly
 262 decreased, which follows the general perception of Kurtosis as being highly
 263 affected by the outliers in data.

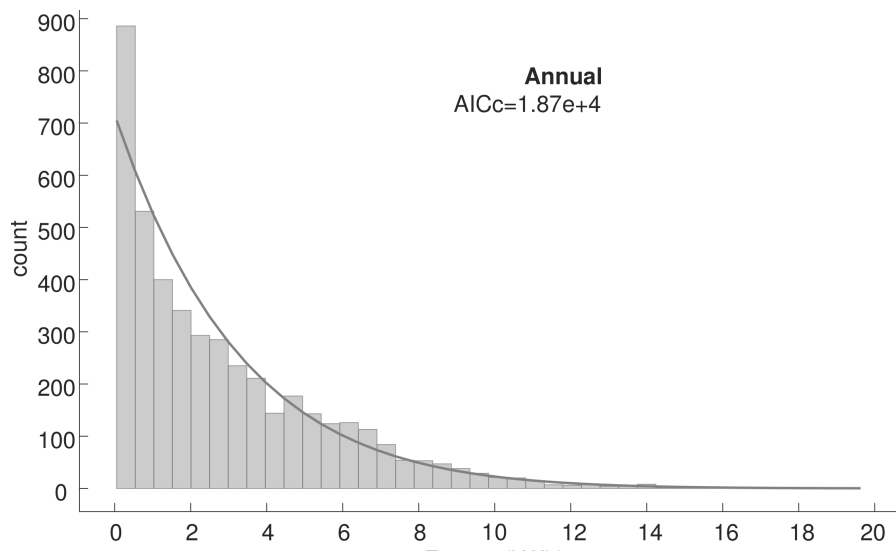
Table 1: General statistics for Energy samples (in kWh) during Delta Solar mode.

Season	Maximum	Minimum	Average	SD (σ)	Skewness	Kurtosis
Autumn	16.1	0.053	2.9	2.7	1.31	4.83
Winter	14.7	0.051	2.5	2.3	1.46	5.48
Spring	163.1 (15.3)	0.05	3.05 (2.92)	5.21 (2.68)	22.70 (1.13)	693.499 (4.04)
Summer	19.6	0.052	3.4	3.13	1.22	4.25
Annual	163.1 (19.6)	0.05	2.9	3.63 (2.71)	20.02 (1.32)	861.63 (4.79)

264 According to Table. 1, maximum discharging event in terms of energy oc-
 265 curred in summer, where the average and SD values are the highest. Among
 266 all seasons, winter shows the most random behaviour because of the highest
 267 Kurtosis. The average value is the lowest in winter and autumn, which is
 268 not surprising as the sunlight intensity is less in these seasons. From energy
 269 perspective, a battery bank of 21.7 kWh capacity (considering 90% round-



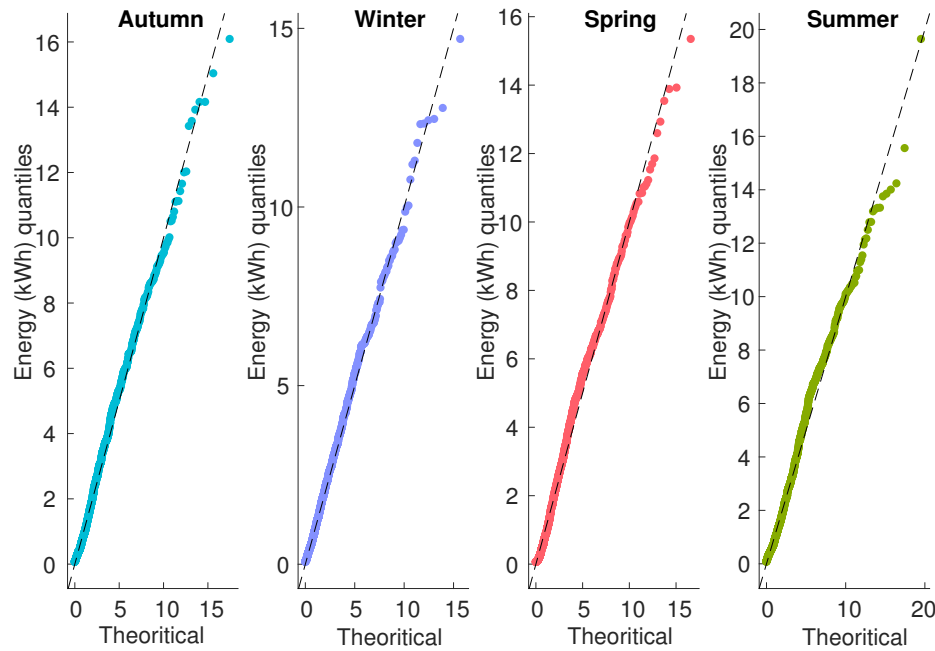
(a) Seasonal



(b) Annual

Figure 3: Histogram of energy samples without outlier

1
 2
 3
 4
 5
 6
 7
 8
 9 trip efficiency for the battery) would be sufficient to successfully compensate
 10 ramp-down events. In other words, this observation defines an upper limit
 11 the kWh capacity of the battery in a sizing study, which statistically would
 12 be able to compensate all ramp-down incidents. Based on this observation,
 13 it can be concluded that an appropriate operational algorithm should pre-
 14 serve at least 21.7 kWh energy in the battery at all times to effectively ride
 15 through ramp-down events, when they occur.
 16
 17



45 Figure 4: Q-Q plot for energy samples based on “Generalised Pareto” DF
 46
 47

48 Additionally, it can be inferred from non-zero skewness in all seasons that
 49 statistical behaviour of the samples is not following a normal distribution
 50 closely. While considering only ramp-down events might seem to cause the
 51 non-normal behaviour, it will be shown in Subsection 4.5 that it is true when
 52 both ramp-up and ramp-down events are considered. This further has been
 53
 54
 55
 56
 57
 58
 59
 60
 61
 62
 63
 64
 65

1
2
3
4
5
6
7
8
9 282 verified by fitting the best density function (DF) on the experimental data,
10 283 as shown in Fig. 3. It contradicts with many papers in this area, which
11 284 assumed normal distribution of ramp events in their analysis [13, 14].
12
13
14

15 285 Seasonal and annual histogram of the battery energy, without outlier, are
16 286 shown in Fig. 3a and 3b, respectively, along with the best DFs. In all cases,
17 287 “Generalized Pareto” found to yield the best fit on the experimental samples.
18
19 288 To further show that the samples are not following a normal distribution,
20 289 seasonal Q-Q plot is shown in Fig. 4 for “Generalised Pareto” DF. It can
21 290 be seen that the field data is following the DF very well. The larger values
22 291 seem to deviate from the DF, which shows a longer tail in the distribution.
23
24 292 The AICc values of the fitted DFs are printed on the figure. One important
25 293 observation from the AICc values is that partitioning experimental data into
26 294 different seasons yields better statistical models.
27
28
29
30
31
32
33

34 295 According to Fig. 3, there are many discharging instances with very low
35 296 energy (as low as 0.05 kWh). Small discharge events can adversely influence
36 297 battery lifetime due to memory effect, as described in [26]. Using super-
37 298 capacitor alongside battery can mitigate these events properly. According to
38 299 [27], super-capacitor size in a hybrid storage system can be calculated by:
39
40
41
42
43

$$C_{sc} = \frac{4 \max(|E_{sc}|)}{v_{sc,max}^2 - v_{sc,min}^2} \quad (4)$$

44 300 where E_{sc} is the maximum energy in Joules; $v_{sc,max}$ and $v_{sc,min}$ are the maximum
45 301 and minimum operational voltages of the super-capacitor; and C_{sc} is the
46 302 capacity in Farads. Since the battery’s inverter operates within 576~748 V
47 303 range on the DC side, the same operational voltages are assumed for super-
48 304 capacitor, i.e., $v_{sc,max} = 748$ and $v_{sc,min} = 576$. Considering that voltage of a
49 305 super-capacitor’s cell is typically between 2.3 to 2.75 Vdc [28], 272 cells are
50
51
52
53
54
55
56
57
58
59
60
61
62
63
64
65

1
 2
 3
 4
 5
 6
 7
 8
 9 306 needed in series to raise the voltage to the desired level. If it is intended
 10 307 to cover 50th percentile of ramp-down energy by super-capacitor (i.e., 2.1
 11 308 kWh which is about 7.56 MJ), then a 33.2 F super-capacitor is required.
 12
 13 309 This is the amount of energy which super-capacitor should deliver during
 14 310 several minutes. However, energy delivery duration in capacitors depends on
 15 311 the capacity and equivalent series resistance (ESR), R_{ESR} , of the capacitor
 16 312 (excluding external resistances):
 17
 18
 19
 20
 21

22
 23
 24
$$\tau = R_{ESR} \cdot C_{sc} \quad (5)$$

 25
 26

27 313 where 1τ is the time that takes a capacitor to discharge to 36.8% of its final
 28 314 voltage. Since it is assumed that the super-capacitor can only be discharged
 29 315 up to 50% of its final voltage, according to [27]:
 30
 31
 32

33
 34
$$C_{sc} = \frac{36.8}{50} \cdot \frac{\tau}{R_{ESR,cell} \times N_s} \quad (6)$$

 35
 36

37 316 where $\tau = 60$ seconds for 50th percentile of the unique events' duration; $R_{ESR,cell}$
 38 317 is about 1 $m\Omega$ per cell for modern super-capacitors; and N_s is the number of
 39 318 cells in series (272 in this study). By doing the calculation, battery capacity
 40 319 should be at least 162.3 F. In Section 4.2, the required power will also be
 41 320 determined.
 42
 43

44 321 If super-capacitor was used for the one year of the experimental data at
 45 322 hand, 1.86 MWh of energy throughput (about 14.5% of total energy delivered
 46 323 by the battery) could have been provided by the super-capacitor. It also
 47 324 could have released the battery from operating in **Delta Solar** mode for
 48 325 2,235 minutes (worth of 1 day, 13 hours, and 15 minutes) to operate in
 49 326 other modes to provide other services to the plant. Moreover, it could have
 50
 51
 52
 53
 54
 55
 56
 57
 58

1
2
3
4
5
6
7
8
9 327 extended the battery lifetime by avoiding partial discharges and reducing
10
11 328 accumulated energy throughput.

12
13
14 329 *4.2. Power*
15

16 330 Besides the energy extracted from the battery, the charge/discharge power
17
18 331 magnitude is an important factor on the battery degradation. It also plays
19
20 332 an inevitable part in any sizing and operation study [20, 25]. Therefore, dis-
21
22 333 charge power magnitude, averaged per minute, is considered for investigation
23
24 334 in this subsection. General statistics of the battery power in **Delta Solar**
25
26 335 mode are derived for annual data as well as different seasons, reported in
27
28 336 Table 2. Seasonal and annual frequency histograms of the samples are also
29
30 337 shown in Fig. 5a and 5b, respectively. Important remarks from the figures
31
32 338 and the table are summarised below:

33
34 Table 2: General statistics of power samples (in kW) during **Delta Solar** mode.
35

36
37
38
39
40
41
42
43
44
45
46
47

Season	Maximum	Average	SD (σ)	Skewness	Kurtosis
Autumn	301.9	95.0	70.6	0.66	2.53
Winter	312.0	87.0	67.8	0.85	2.94
Spring	325.4	101.8	80.1	0.66	2.39
Summer	331.2	110.1	80.6	0.62	2.37
Annual	331.2	98.2	75.4	0.72	2.59

48
49
50 339 • Similar to the energy samples, the experimental power samples are best
51
52 340 modelled using “Generalised Pareto”. The largest incident occurred in sum-
53
54 341 mer, similar to the energy values, where power magnitude was 331.2 kW.
55
56 342 Summer also experiences higher ramp-down power on average whereas winter

1
2
3
4
5
6
7
8
9 343 has the lowest average value. Winter, however, represents more stochastic
10 344 behaviour compared to the other seasons because of higher Skewness and
11 345 Kurtosis. These observations are aligned with those inferred from the energy
12 346 samples in the previous subsection.

13 347 • DFs fitted on the seasonal data are more accurate compared to those ones
14 348 fitted on the annual samples based on the AICs values given in Fig. 5. As
15 349 shown in the analyses so far, partitioning data into different clusters (e.g.,
16 350 seasons) have a considerable impact on the accuracy of the statistical models.
17 351 So far, it is shown that seasonality pattern exists in the battery operational
18 352 data. However, it is worth to use clustering techniques to identify different
19 353 categories in data beyond seasonality, and to fit more appropriate DF on
20 354 every cluster. This way, more accurate models can be developed from the
21 355 experimental data, which will be useful in the battery sizing and operation
22 356 studies in the future.

23 357 • In general, it is more difficult to statistically model the battery power dur-
24 358 ing ramp-down events compared to the energy samples. This further means
25 359 that a larger error should be anticipated for power in sizing or operation
26 360 studies, e.g., when predicting power for real-time operation.

27 361 • 86th percentile has power equal or less than 150 kW, which is half of the
28 362 battery rated capacity. This is good for battery health since high-power
29 363 incidents have occurred less frequently over the year.

30 364 In Fig. 6, the maximum power of every unique event is plotted against
31 365 the accumulated energy of the same event. It can be seen that there is
32 366 almost a linear relationship between the two parameters. Essentially, the
33 367 high-power incidents coincide with the high-energy events. The correlation

coefficients for seasonal and annual samples are given in the caption, which
emphasizes on the existence of a linear correlation between the two parameters.
It also means that a joint probability distribution between the energy and
power samples might better capture variations in the two random parameters.
While the correlation coefficients of the seasonal and annual values are fairly
close, slope of the line is not similar in all seasons. Therefore, accuracy of the
modelling (in terms of joint DF or cumulative distribution function (CDF))
will essentially improve if data is partitioned seasonally.

Besides power, rate of change of power (RoCoP) has significant impacts
on the battery lifetime. This is a well-known fact that highly fluctuating
charge and discharge regime can degrade battery faster [29]. RoCoP for every
unique incident is calculated in this study, seasonal and annual histograms
of which are shown in Fig. 7a and 7b, respectively. Negative values show
a drop in power with respect to the previous time instance. It can be seen
from Fig. 7 that the number of incidents close to zero is disproportionately
bigger than other range of values (i.e., bins), which could be another evidence
supporting hybrid energy system application. The application can further be
justified by the observation made from Fig. 6, in which low-energy incidents
correlate with low-power magnitude most of the time.

General statistics of the RoCoP samples are given in Table 3 for seasonal
and annual data. It can be seen that RoCoP can be as high as nominal
power of battery. This sort of power fluctuation is strenuous on the bat-
tery with significant consequences on its lifetime. Similar to the energy and
power samples, the largest RoCoP values occur in summer. However, the
average and SD values are bigger in spring. That being said, winter with

1
 2
 3
 4
 5
 6
 7
 8
 9 393 highest Skewness and Kurtosis is the most unpredictable season for the Ro-
 10
 11 394 CoP modelling, which is similar to what have been observed for the energy
 12
 13 395 and power samples.
 14

15 Table 3: General statistics of RoCoP samples (in kW/min) during **Delta Solar** mode.
 16

Season	Maximum	Average	SD (σ)	Skewness	Kurtosis
Autumn	265.3	83.0	101.95	0.202	2.57
winter	296.0	82.13	102.69	0.254	2.80
Spring	293.98	96.09	118.7	0.22	2.40
Summer	307.08	95.49	114.89	0.21	2.37
Annual	307.08	89.33	110.05	0.22	2.54

30
 31 396 To finalise super-capacitor sizing from Section 4.1, power requirement
 32
 33 397 of the hypothetical super-capacitor is calculated. Nominal power of super-
 34
 35 398 capacitors is specified in kW/kg. This value changes from one model and
 36
 37 399 manufacturer to another. Therefore, power sizing of the super-capacitor de-
 38
 39 400 pends on the specific model that is going to be used in an application. If
 40
 41 401 it was intended to use a BCAP0650 super-capacitor (650 F) from Maxwell
 42
 43 402 Company [30] for the Gatton plant, which has specific power of 6.8 kW/kg
 44
 45 403 and each cell is about 200 g, it can handle power up to 369.9 kW which is
 46
 47 404 higher than maximum power of each battery inverter and bank. Moreover,
 48
 49 405 the maximum power incident over a year never exceeded 331.2 kW (accord-
 50
 51 406 ing to Table 2), which is still below nominal power of the super-capacitor.
 52
 53 407 Therefore, power as well as energy requirements can be fulfilled by selecting
 54
 55 408 BCAP0650 super-capacitor from Maxwell company. According to [30], the
 56
 57 409 price of this model of super-capacitor is about AU\$57 per cell and the overall
 58
 59
 60
 61
 62
 63
 64
 65

1
2
3
4
5
6
7
8
9 410 cost of the super-capacitor for this application will be less than AU\$16,000.
10
11 411 Please note that the cost of power electronic interface and controller is not
12
13 412 considered.
14
15
16 413 *4.3. Battery SOC*
17
18
19 414 Battery SOC at the end of each ramp-down event is another important
20 415 parameter in the battery health and sizing studies. SOC values are shown
21 416 in Fig. 8 at the end of each unique event for different seasons as well as the
22 417 whole year. General statistics of the SOC samples are also reported in Ta-
23 418 ble 4 for different seasons and annual data. In general, the battery SOC is
24 419 well-maintained within an acceptable range in different seasons. The max-
25 420 imum SOC is almost the same in all seasons and it is very high. It shows
26 421 that there are low energy events which might be better to be covered by
27 422 other storage devices, such as super-capacitor. In summer, we have the best
28 423 operation scenario for battery since the SOC values never go below 65% and
29 424 the average SOC is the highest at about 85%. In this case, the battery
30 425 will be ready for the future events in terms of available energy . It is an-
31 426 ticipated because summer has the highest amount of solar irradiation and
32 427 longer daylight hours so that battery has more opportunity to be charged.
33
34
35
36
37
38
39
40
41
42
43
44
45
46
47
48
49
50
51
52
53
54
55
56
57
58
59
60
61
62
63
64
65

1
2
3
4
5
6
7
8
9 435 Skewness, the battery SOC shows negative Skewness, which implies a longer
10
11 436 tail on the left. This is because of low SOC incidents in the samples.
12
13
14

Table 4: General statistics of battery SOC samples (in %) during **Delta Solar** mode.

Season	Maximum	Minimum	Average	SD (σ)	Skewness	Kurtosis
Autumn	99.0	9.9	75.7	14.45	-0.71	4.09
winter	96.6	15.2	73.86	14.24	-0.71	3.85
Spring	97.5	22.4	82.24	9.14	-1.18	6.21
Summer	98.6	65.2	84.72	7.19	-0.17	2.25
Annual	99.0	9.9	79.11	12.46	-1.13	5.20

28
29
30 437 Figure. 9 shows the seasonal and annual histograms of the SOC exper-
31 imental data and the best DF fitted. Most of the values are in the upper
32 range of SOC, which is good for battery health. While there was always a
33
34 438 single DF, which could accurately model the seasonal and annual data for the
35 energy and power samples, different DFs found to model SOC experimental
36 data the best. Furthermore, the energy and power experimental data were
37
38 439 fitting well on unimodal distribution. However, the SOC samples, specially
40
41 440 in autumn and winter, represents bimodal distribution with two peaks. Nev-
42
43 441 ertheless, the importance of data partitioning (specifically based on different
44 seasons) can be realised from SOC histograms. For histogram and DF fitting,
45
46 442 data are centred around their average value because it yields better fit. The
47
48 443 average SOC was 79.11% from all available data.
49
50
51
52
53
54
55
56
57
58
59
60
61
62
63
64
65

1
2
3
4
5
6
7
8
9 449 *4.4. Time Gap*
10

11 450 After every ramp-down incident, the battery energy will reduce. Hence,
12 451 there should be enough time to charge the battery for the future events if
13 452 battery energy is depleted. It will have significant consequences in the sizing
14 453 and operation studies. For instance, if incidents are too close, it leads to a
15 454 larger battery capacity to cover next incident in line. The time gap between
16 455 two events can be problematic when it is too short to charge the battery until
17 456 the next event. It depends on the battery SOC at the beginning of every
18 457 event, capacity of the battery, and the energy required for the next event,
19 458 $f(SOC_{init}, E_{batt}, E_{next})$.
20
21
22
23
24
25
26
27

28 459 To analyse this parameter, the time difference between the unique events
29 460 is calculated from the data, general statistics of which is reported in Table 5.
30
31 461 The first event of every day is not considered in this analysis. The max-
32 462 imum time gap in winter and spring are larger than their counterparts in
33 463 other two seasons. However, the average time gap is larger in autumn which
34 464 implies fewer incidents throughout the season. The time gap in winter is
35 465 more stochastic because of high Kurtosis value. This observation suggests
36 466 different operation algorithms for battery in different seasons to improve the
37 467 battery performance and health. The 50th percentile of the time gap samples
38 468 is 5 minutes, which means that the time gap is 5 minutes or less for 50%
39 469 of the time. This could have significant impacts on the battery sizing and
40 470 operation studies. Similar to the energy and power samples, the time gap
41 471 can be best modelled with “Generalised Pareto” DF for every season as well
42 472 as the annual samples.
43
44
45
46
47
48
49
50
51
52
53
54
55
56
57
58
59
60
61
62
63
64
65

1
2
3
4
5
6
7
8
9
10
11
12
13
14
15
16
17
18
19
20
21
22
23
24
25
26
27
28
29
30
31
32
33
34
35
36
37
38
39
40
41
42
43
44
45
46
47
48
49
50
51
52
53
54
55
56
57
58
59
60
61
62
63
64
65

Table 5: General statistics of time gap samples (in minute) between consecutive events during **Delta Solar** mode.

Season	Maximum	Minimum	Average	SD (σ)	Skewness	Kurtosis
Autumn	370	2	16.1	33.4	6.3	53.8
Winter	388	2	12.1	26.2	7.7	81.6
Spring	400	2	12.8	27.8	7.2	74.5
Summer	367	2	13.0	27.0	7.2	74.0
Annual	400	2	13.4	28.8	7.1	69.5

473 *4.5. PV-side Ramp-Rate Analysis*

474 So far, only ramp-down control was investigated using battery operation
 475 data, where commands sent by the CSS has been followed by the battery
 476 inverter controller. The observations presented in this subsection could be
 477 useful in battery sizing studies, which typically starts from predicting PV
 478 plant. To do the analyses, data are collected for each PV string, shown in
 479 Fig. 1, on both DC and AC sides of the inverters. Ramp-rate for the entire
 480 PV generation is limited to 10 kW/s (i.e., 600 kW/min). To analyse PV
 481 strings individually, ramp-rate limit is divided between five arrays according
 482 to their rated capacity. Values are normalised based on the maximum power
 483 on the DC side of the inverter, i.e., 684 kW, for comparison purposes. Also,
 484 total PV plant production is simply calculated by adding generation of the
 485 five PV arrays.

486 As expected, there is 100% correlation between DC and AC values of
 487 every inverter. The number of ramp-rate violations, maximum, average of
 488 absolute values, and SD of violations are plotted in Fig. 10 for every PV

1
2
3
4
5
6
7
8
9 489 array and the overall plant. Values are given for both DC and AC sides of
10
11 490 every inverter for comparison.

12 491 Following observations can be made from Fig. 10:

13
14
15 492 • For all PV arrays and the overall plant production, it can be seen that
16
17 493 the ramp-rate violations on the DC side is always more than the AC
18
19 494 side of the inverter. This is mainly caused by the inverter losses and
20
21 495 reactive power compensation, as explained in Section 2. In the battery
22
23 496 sizing and operation studies, these factors are typically ignored.

24
25
26 497 • PV plant smoothing effect can be realised from the figure where the
27
28 498 number of ramp-rate violations, maximum, average, and SD of violations
29
30 499 are significantly less for overall plant production compared to
31
32 500 the individual PV array performance. In theoretical studies reported
33
34 501 in the literature, the model of a single PV module is usually used to
35
36 502 generate PV power time series from solar irradiation and ambient tem-
37
38 503 perature data to calculate ramp events. It is clear from Fig. 10 that
39
40 504 neglecting smoothing effect in those studies leads to wrong decisions,
41
42 505 e.g., over-sized battery capacity in sizing studies.

43
44
45 506 • SA and DA arrays have the largest maximum ramp incidents. Also,
46
47 507 the average ramp-rate violations is the highest for the SA and DA
48
49 508 arrays. It shows that although advanced tracking systems increase
50
51 509 overall generation in the plant, they require more efforts to control
52
53 510 ramping events (e.g., larger storage).

54
55
56 511 • “Generalised Extreme Value” DF found to be the best for modelling the
57
58 512 ramp-rate events (combination of ramp-up and ramp-down). There-

1
2
3
4
5
6
7
8
9 513 fore, using normal distribution for such application will lead to signifi-
10 514 cant error in calculations and modelling.
11
12
13
14
15
16
17
18
19
20
21
22
23
24
25
26
27
28
29
30
31
32
33
34
35
36 521

- 515 • The maximum ramp-rate violation can be as high as the rated capacity
516 of the individual PV array. For the overall plant, it is still higher
517 than 85%, which is significant. Additionally, the average ramp-rate
518 violation for the overall plant is not significantly different from the
519 individual arrays. While the smoothing effect can reduce the number
520 of ramp events, it might not be as much effective during large ramping
521 incidents.
- 522 • Compared to the maximum ramp-rate violations, the average and SD
523 values are relatively small. It proves that severe ramping incidents
524 rarely occurred. Therefore, appropriate statistical model of the ramp
525 events is needed to properly size and operate battery.

37 526 Ramp-up and ramp-down incidents are separately analysed in Fig. 11 for
38 527 the AC side of the inverter for all PV arrays. The following insights can be
39 528 inferred from the experimental data shown in Fig. 11:

40
41
42 529

- 43 530 • Despite the PV inverter effort to regulate ramp-up events and reactive
44 531 power compensation, the number of ramp-up incidents is significantly
45 532 more than ramp-down ones in the individual arrays. It suggests that
46 533 the ramp-up events happen more often than the ramp-down ones. It
47 534 will have consequences in the battery sizing and operation studies.
- 48 535 • While both ramp-up and ramp-down events are considerably reduced
49 536 at the entire plant level, the smoothing effect has more impact on the
50 537 ramp-up incidents compared to the ramp-down events.

1
2
3
4
5
6
7
8
9
10
11
12
13
14
15
16
17
18
19
20
21
22
23
24
25
26
27
28
29
30
31
32
33
34
35
36
37
38
39
40
41
42
43
44
45
46
47
48
49
50
51
52
53
54
55
56
57
58
59
60
61
62
63
64
65

- 537 • Although the number of incidents is more for the ramp-up events, maximum, average, and SD of violations for all cases occurred during the ramp-down incidents. Higher average of the ramp-down events means that the battery is more likely to be discharged rather than charged. Therefore, battery should always maintain a high level of charge to be able to ride through the ramp-down events by being regularly charged.
- 543 • The previous observation also shows that ramp-up and ramp-down events are not energy neutral, i.e., accumulated charged and discharged energy during ramping incidents are not equal. Therefore, the battery operation algorithm should take this into account by regularly charging the battery.
- 548 • It can also be seen from Fig. 11 that SD is bigger for the ramp-down events, which makes it less predictable.

550 These observations are useful for the next generation of the sizing studies
551 and designing battery operation algorithms.

552 5. Conclusion

553 This paper offers thorough analyses of the battery operation under ramp-
554 down control mode within a medium-scale PV plant. One year of field data
555 is used to draw insights from the battery operation, which could be useful for
556 the battery sizing and operational studies in the future. Investigations are
557 carried out for the different parameters of the battery operation. It has been
558 shown that seasonality has an impact on the ramp events, which consequently
559 affect the battery operation in different ways, such as SOC level. As a result,

1
2
3
4
5
6
7
8
9 560 statistical model of different parameters are more accurate when modelling
10 561 is carried out on the seasonal data. According to the statistical analyses,
11 562 the battery energy is more predictable compared to the battery power, while
12 563 there is a strong correlation between the two parameters. The application of
13 564 super-capacitor is also assessed, which showed that it can improve battery
14 565 lifetime and the economic operation of the whole plant. Analysing parame-
15 566 ters such as the time gap between two consecutive events revealed that they
16 567 should be considered in the sizing and operation studies.

24 568 Finally, investigation on the ramp events on the DC and AC sides of the
25 569 PV inverters shows that using theoretical model of PV module without ac-
26 570 counting for smoothing effects in medium- and large-scale PV plants, inverter
27 571 operation for reactive power consumption, system-wide losses, etc., can lead
28 572 to wrong decisions in the sizing and operation studies. It is also shown that
29 573 smoothing effect is not an ultimate solution to the PV ramp-rate problem.

37 574 **Acknowledgment**

38 575 This work was performed in part using equipment and infrastructure
39 576 funded by the Australian Federal Governments Department of Education
40 577 AGL Solar PV Education Investment Fund Research Infrastructure Project.
41 578 The University of Queensland is the Lead Research Organisation in partner-
42 579 ship with AGL, First Solar and the University of New South Wales.

51 580 **References**

52 581 [1] A. P. Institute, “Australian pv market since april 2001.” <http://pv-map.apvi.org.au/analyses#top>. Accessed: 2017-10-10.

1
2
3
4
5
6
7
8
9 583 [2] C. E. Council, "Clean energy australia report 2016," tech. rep., Clean
10
11 584 Energy Council, 2016.

12
13
14 585 [3] R. Shah, N. Mithulanathan, R. Bansal, and V. Ramachandaramurthy,
15
16 "A review of key power system stability challenges for large-scale pv inte-
17
18 587 gration," *Renewable and Sustainable Energy Reviews*, vol. 41, pp. 1423–
19
20 588 1436, 2015.

21
22
23 589 [4] T. Jamal, T. Urmee, M. Calais, G. Shafiqullah, and C. Carter, "Technical
24
25 challenges of pv deployment into remote australian electricity networks:
26
27 591 A review," *Renewable and Sustainable Energy Reviews*, 2017.

28
29
30 592 [5] K. Lappalainen and S. Valkealahti, "Output power variation of different
31
32 593 pv array configurations during irradiance transitions caused by moving
33
34 594 clouds," *Applied Energy*, vol. 190, pp. 902–910, 2017.

35
36
37 595 [6] V. Garrone, M. Hibbert, J. Mayer, C. Froome, S. Goodwin, and
38
39 596 P. Meredith, "Technical requirements for the connection of a mw-scale
40
41 597 pv array with battery storage to an 11 kv feeder in queensland," in
42
43 598 *Asia-Pacific Solar Research Conf*, 2014.

44
45
46 599 [7] J. Marcos, O. Storkël, L. Marroyo, M. Garcia, and E. Lorenzo, "Storage
47
48 600 requirements for pv power ramp-rate control," *Solar Energy*, vol. 99,
49
50 601 pp. 28–35, 2014.

51
52
53 602 [8] S. Shivashankar, S. Mekhilef, H. Mokhlis, and M. Karimi, "Mitigating
54
55 603 methods of power fluctuation of photovoltaic (pv) sources—a review," *Re-
56
57 604 newable and Sustainable Energy Reviews*, vol. 59, pp. 1170–1184, 2016.

1
2
3
4
5
6
7
8
9
10
11
12
13
14
15
16
17
18
19
20
21
22
23
24
25
26
27
28
29
30
31
32
33
34
35
36
37
38
39
40
41
42
43
44
45
46
47
48
49
50
51
52
53
54
55
56
57
58
59
60
61
62
63
64
65

- [9] R. Yan and T. K. Saha, “Power ramp rate control for grid connected photovoltaic system,” in *IPEC, 2010 Conference Proceedings*, pp. 83–88, IEEE, 2010.
- [10] X. Chen, Y. Du, and H. Wen, “Forecasting based power ramp-rate control for pv systems without energy storage,” in *Future Energy Electronics Conference and ECCE Asia (IFEEC 2017-ECCE Asia), 2017 IEEE 3rd International*, pp. 733–738, IEEE, 2017.
- [11] R. K. Lam and H.-G. Yeh, “Pv ramp limiting controls with adaptive smoothing filter through a battery energy storage system,” in *Green Energy and Systems Conference (IGESC), 2014 IEEE*, pp. 55–60, IEEE, 2014.
- [12] J. Marcos, I. de la Parra, M. García, and L. Marroyo, “Control strategies to smooth short-term power fluctuations in large photovoltaic plants using battery storage systems,” *Energies*, vol. 7, no. 10, pp. 6593–6619, 2014.
- [13] A. Puri, “Optimally smoothing output of pv farms,” in *PES General Meeting— Conference & Exposition, 2014 IEEE*, pp. 1–5, IEEE, 2014.
- [14] A. K. Barnes, J. C. Balda, and A. Escobar-Mejía, “A semi-markov model for control of energy storage in utility grids and microgrids with pv generation,” *IEEE Transactions on Sustainable Energy*, vol. 6, no. 2, pp. 546–556, 2015.
- [15] I. De la Parra, J. Marcos, M. García, and L. Marroyo, “Storage re-

1
2
3
4
5
6
7
8
9
10
11
12
13
14
15
16
17
18
19
20
21
22
23
24
25
26
27
28
29
30
31
32
33
34
35
36
37
38
39
40
41
42
43
44
45
46
47
48
49
50
51
52
53
54
55
56
57
58
59
60
61
62
63
64
65

627 requirements for pv power ramp-rate control in a pv fleet," *Solar Energy*,
628 vol. 118, pp. 426–440, 2015.

629 [16] R. van Haaren, M. Morjaria, and V. Fthenakis, "An energy storage al-
630 gorithm for ramp rate control of utility scale pv (photovoltaics) plants,"
631 *Energy*, vol. 91, pp. 894–902, 2015.

632 [17] M. J. Reno, M. Lave, J. E. Quiroz, and R. J. Broderick, "Pv ramp rate
633 smoothing using energy storage to mitigate increased voltage regulator
634 tapping," in *Photovoltaic Specialists Conference (PVSC), 2016 IEEE*
635 43rd, pp. 2015–2020, IEEE, 2016.

636 [18] M. Garcia-Plaza, J. E.-G. Carrasco, J. Alonso-Martinez, and A. P. Asen-
637 sio, "Battery energy storage system in smoothing control application of
638 photovoltaic power fluctuations caused by clouds passing," in *Industrial*
639 *Electronics Society, IECON 2016-42nd Annual Conference of the IEEE*,
640 pp. 1992–1997, IEEE, 2016.

641 [19] A. Puri, "Bounds on the smoothing of renewable sources," in *Power &*
642 *Energy Society General Meeting, 2015 IEEE*, pp. 1–5, IEEE, 2015.

643 [20] A. Makibar, L. Narvarte, and E. Lorenzo, "On the relation between
644 battery size and pv power ramp rate limitation," *Solar Energy*, vol. 142,
645 pp. 182–193, 2017.

646 [21] M. Alam, R. Yan, T. Saha, A. Chidurala, and D. Eghbal, "Learning
647 from a 3.275 mw utility scale pv plant project," *CIGRÉ*, 2016.

648 [22] A. Papoulis, *Probability & statistics*, vol. 2. Prentice-Hall Englewood
649 Cliffs, 1990.

1
2
3
4
5
6
7
8
9
10
11
12
13
14
15
16
17
18
19
20
21
22
23
24
25
26
27
28
29
30
31
32
33
34
35
36
37
38
39
40
41
42
43
44
45
46
47
48
49
50
51
52
53
54
55
56
57
58
59
60
61
62
63
64
65

[23] N. Balakrishnan and W. W. Chen, “Quantile-quantile plots and goodness-of-fit test,” in *Handbook of Tables for Order Statistics from Lognormal Distributions with Applications*, pp. 39–40, Springer, 1999.

[24] D. Freedman and P. Diaconis, “On the histogram as a density estimator: L 2 theory,” *Zeitschrift für Wahrscheinlichkeitstheorie und verwandte Gebiete*, vol. 57, no. 4, pp. 453–476, 1981.

[25] N. Saadat, S. S. Choi, and D. M. Vilathgamuwa, “A statistical evaluation of the capability of distributed renewable generator-energy-storage system in providing load low-voltage ride-through,” *IEEE Transactions on Power Delivery*, vol. 30, no. 3, pp. 1128–1136, 2015.

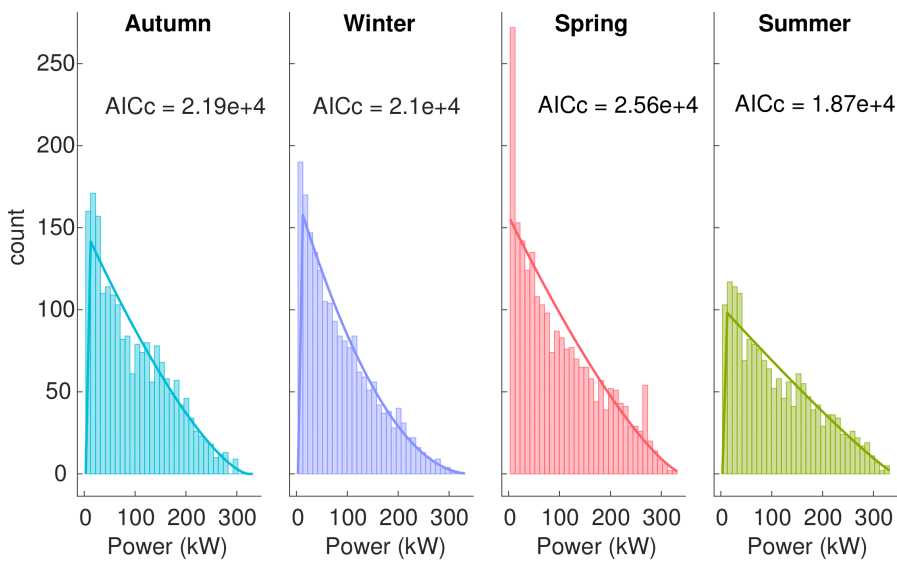
[26] T. Sasaki, Y. Ukyo, and P. Novák, “Memory effect in a lithium-ion battery,” *Nature materials*, vol. 12, no. 6, p. 569, 2013.

[27] D. B. W. Abeywardana, B. Hredzak, V. G. Agelidis, and G. D. Demetriades, “Supercapacitor sizing method for energy-controlled filter-based hybrid energy storage systems,” *IEEE Transactions on Power Electronics*, vol. 32, no. 2, pp. 1626–1637, 2017.

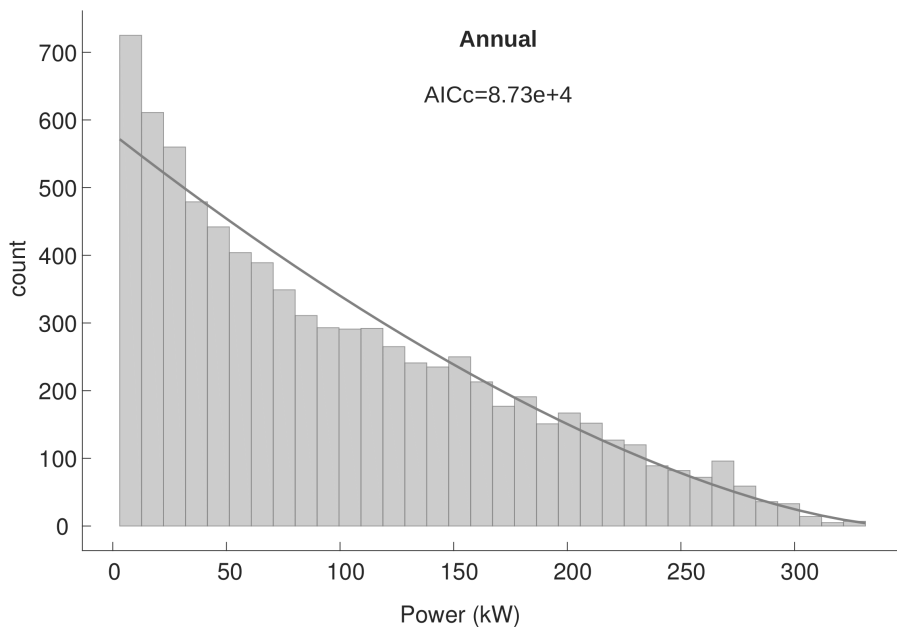
[28] “Bu-209: How does a supercapacitor work?” http://batteryuniversity.com/learn/article/whats_the_role_of_the_supercapacitor. Accessed: 2017-10-05.

[29] K. Uddin, A. D. Moore, A. Barai, and J. Marco, “The effects of high frequency current ripple on electric vehicle battery performance,” *Applied Energy*, vol. 178, pp. 142–154, 2016.

1
2
3
4
5
6
7
8
9 672 [30] “K2 2.7v series documents: High capacity cells.” http://www.maxwell.com/images/documents/K2Series_DS_1015370_5_20141104.pdf. Ac-
10
11 673
12 674 cessed: 2017-10-05.
13
14
15
16
17
18
19
20
21
22
23
24
25
26
27
28
29
30
31
32
33
34
35
36
37
38
39
40
41
42
43
44
45
46
47
48
49
50
51
52
53
54
55
56
57
58
59
60
61
62
63
64
65



(a) Seasonal



(b) Annual

Figure 5: Histogram of the battery power samples during **Delta Solar** mode

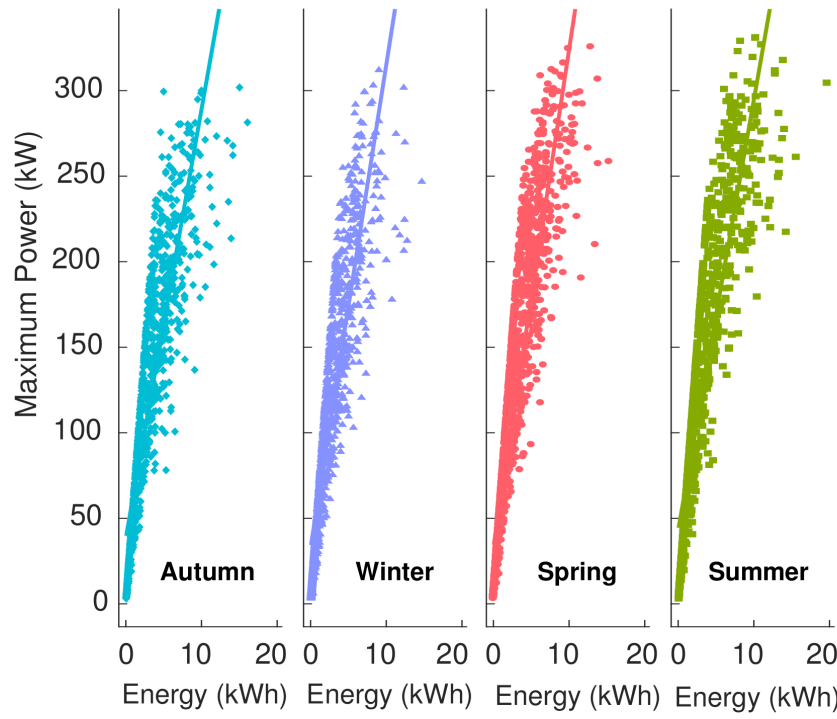
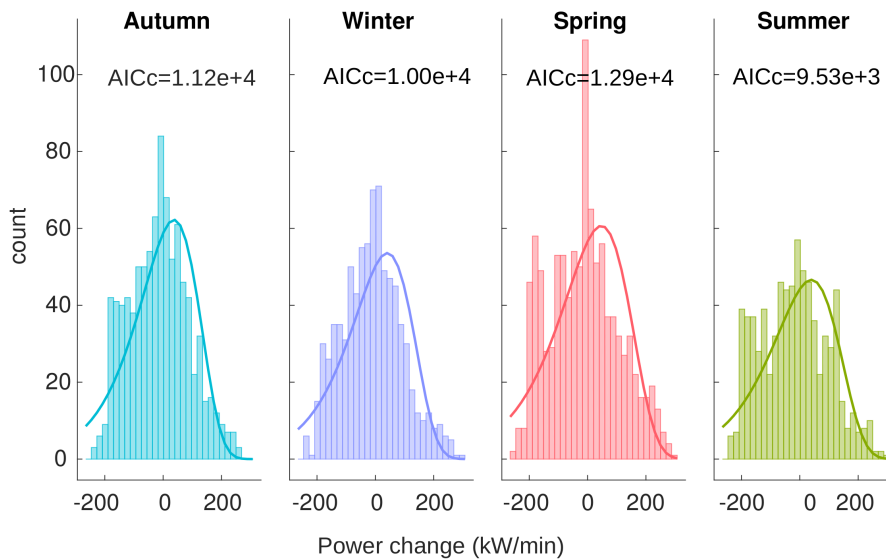
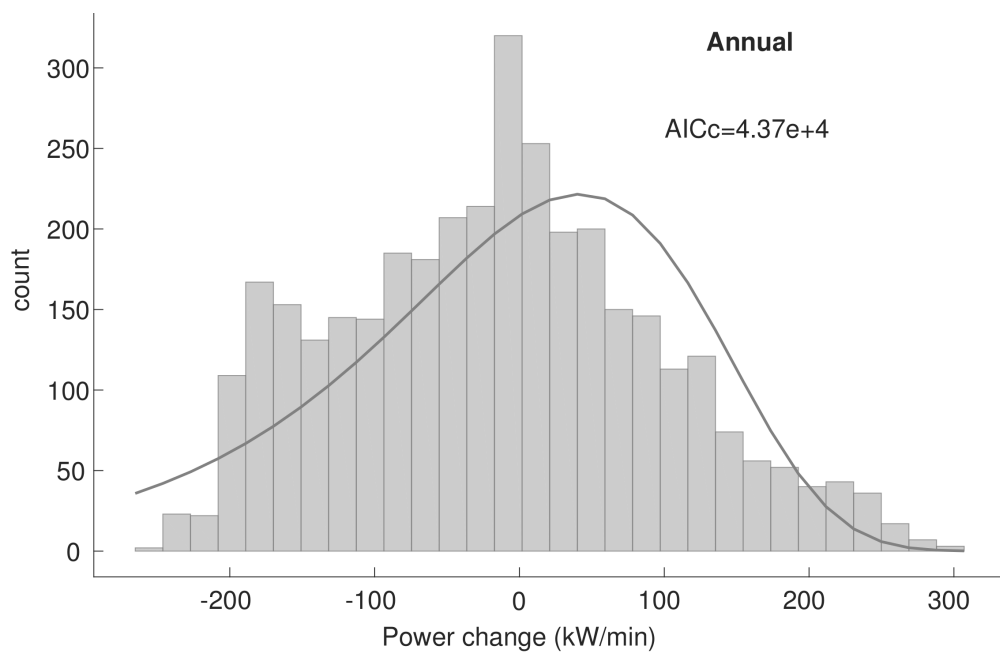


Figure 6: Maximum power vs. energy of every unique incident– Seasonal (*correlation coefficient* (ρ) is 0.88, 0.885, 0.893, and 0.906 for autumn, winter, spring, and summer, respectively) and Annual (ρ is 0.891)



(a) Seasonal



(b) Annual

Figure 7: Histogram of RoCoP samples (kW/min) without outlier

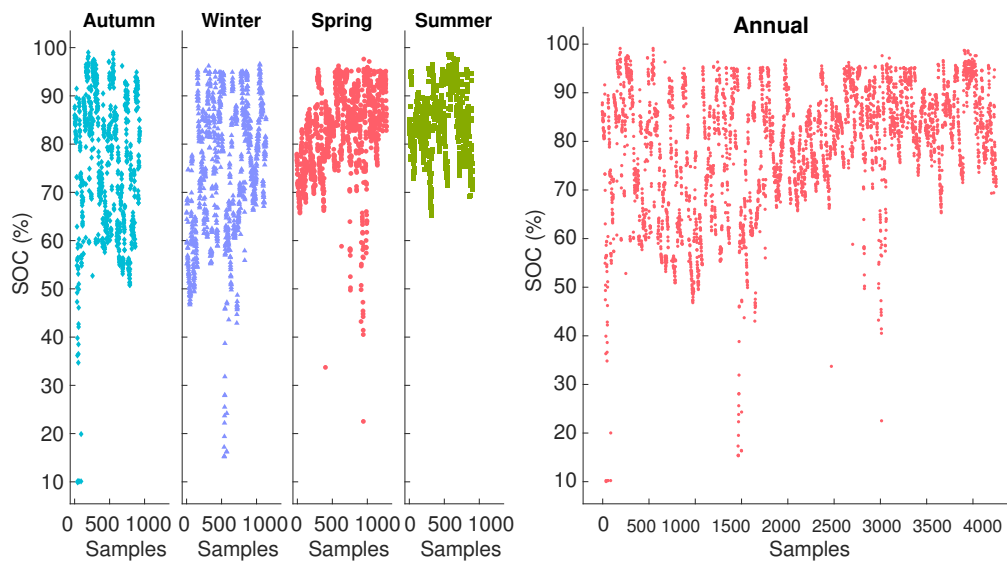
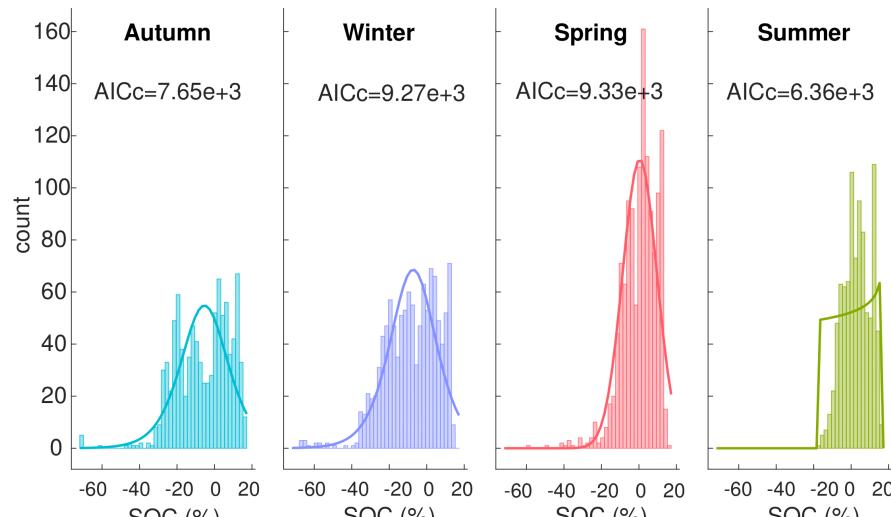
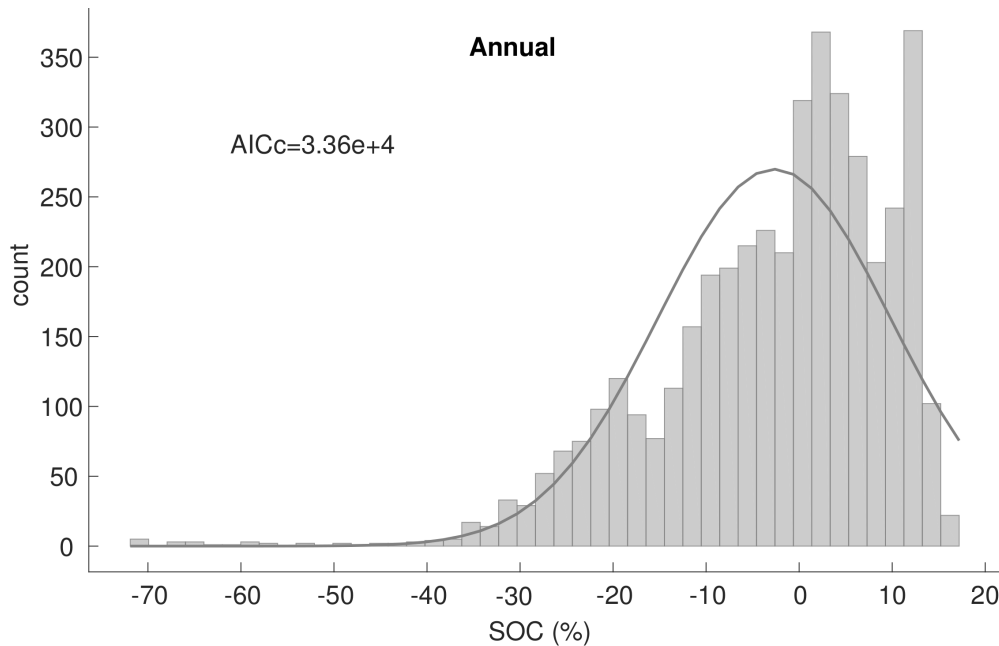


Figure 8: Battery SOC at the end of each unique Delta Solar event



(a) Seasonal



(b) Annual

Figure 9: Histogram of the Battery SOC samples without outlier [Fitted PDF for Autumn: *Logistic*, Winter: *Logistic*, Spring: *Normal*, Summer: *Generalised Pareto*, and Annual: *Normal*]

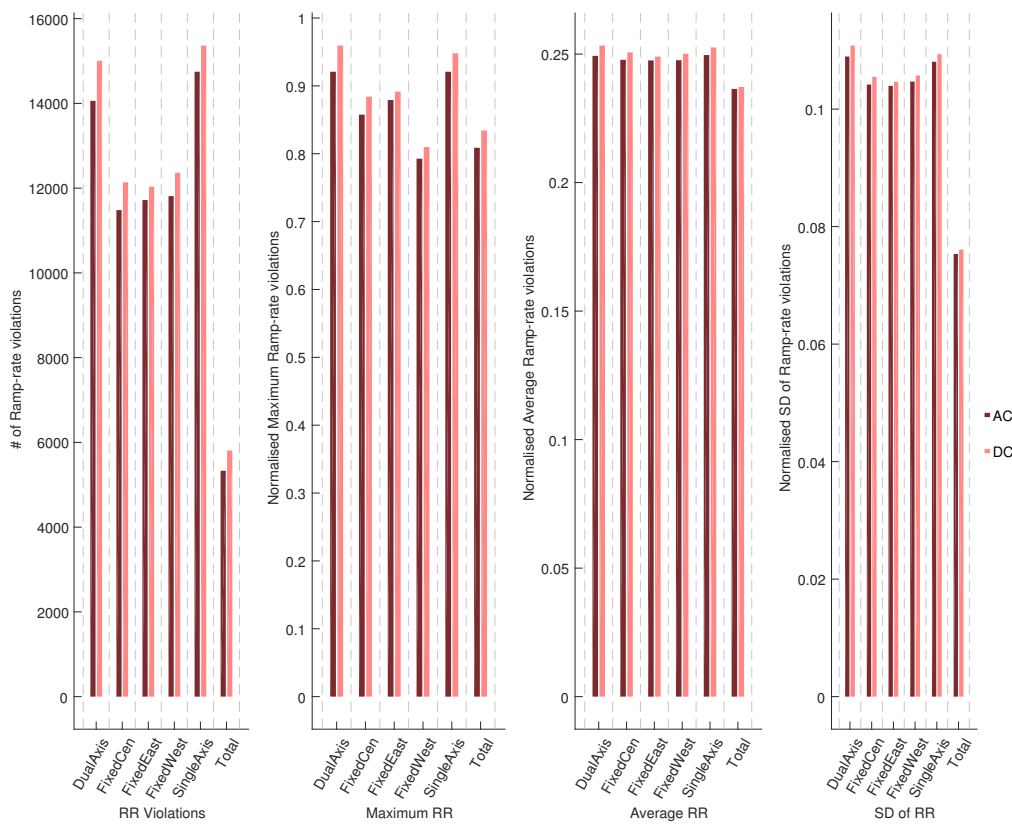
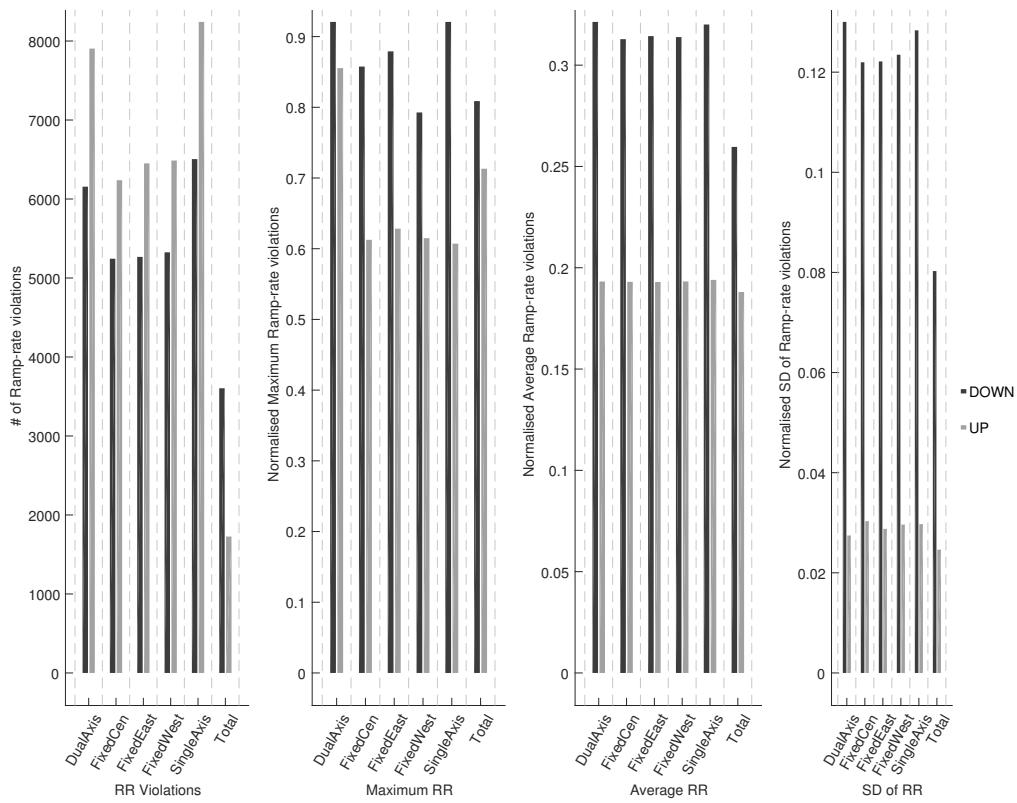


Figure 10: Ramp-rate violations for all PV arrays on DC and AC sides of inverters



46 Figure 11: Ramp-up and ramp-down violations for all PV arrays on the AC side of inverters
47